Temporal refinement of sensory-evoked activity across layers in developing mouse barrel cortex

van der Bourg, Alexander ; Yang, Jenq-Wei ; Stüttgen, Maik C ; Reyes-Puerta, Vicente ; Helmchen, Fritjof ; Luhmann, Heiko J

Abstract: Rhythmic whisking behavior in rodents fully develops during a critical period about 2 weeks after birth, in parallel with the maturation of other sensory modalities and the onset of exploratory locomotion. How whisker-related sensory processing develops during this period in the primary somatosensory cortex (S1) remains poorly understood. Here, we characterized neuronal activity evoked by single- or dual-whisker stimulation patterns in developing S1, before, during and after the occurrence of active whisking. Employing multi-electrode recordings in all layers of barrel cortex in urethane-anesthetized mice, we find layer-specific changes in multi-unit activity for principal and neighboring barrel columns. While whisker stimulation evoked similar early responses (0-50 ms post-stimulus) across development, the late response (50-150 ms post-stimulus) decreased in all layers with age. Furthermore, peak onset times and the duration of the late response decreased in all layers across age groups. Responses to paired-pulse stimulation showed increases in spiking precision and in paired-pulse ratios in all cortical layers during development. Sequential activation of two neighboring whiskers with varying stimulus intervals evoked distinct response profiles in the activated barrel columns, depending on the direction and temporal separation of the stimuli. In conclusion, our findings indicate that the temporal sharpening of sensory-evoked activity coincides with the onset of active whisking.

DOI: https://doi.org/10.1111/ejn.14413

Received: 31 October 2018 | Revised: 5 March 2019 | Accepted: 17 March 2019

DOI: 10.1111/ejn.14413

RESEARCH REPORT

EJN European Journal of Neuroscience FENS WILEY

Temporal refinement of sensory-evoked activity across layers in developing mouse barrel cortex

Alexander van der Bourg[1,2] | Jenq-Wei Yang[3] | Maik C. Stüttgen[4] | Vicente Reyes-Puerta[3] | Fritjof Helmchen[1,2] | Heiko J. Luhmann[3]

[1]Laboratory of Neural Circuit Dynamics, Brain Research Institute, University of Zurich, Zurich, Switzerland

[2]Neuroscience Center Zurich, Zurich, Switzerland

[3]Institute of Physiology, University Medical Center of the Johannes Gutenberg University, Mainz, Germany

[4]Institute of Pathophysiology, University Medical Center of the Johannes Gutenberg University, Mainz, Germany

Correspondence
Heiko J. Luhmann, Institute of Physiology, Duesbergweg 6, University Medical Center of the Johannes Gutenberg University, D-55128 Mainz, Germany.
Email: luhmann@uni-mainz.de

Funding information
Schweizerischer Nationalfonds zur Förderung der Wissenschaftlichen Forschung, Grant/Award Number: SNSF 310030E-147485; Deutsche Forschungsgemeinschaft, Grant/Award Number: DFG FOR1341

Abstract

Rhythmic whisking behavior in rodents fully develops during a critical period about 2 weeks after birth, in parallel with the maturation of other sensory modalities and the onset of exploratory locomotion. How whisker-related sensory processing develops during this period in the primary somatosensory cortex (S1) remains poorly understood. Here, we characterized neuronal activity evoked by single- or dual-whisker stimulation patterns in developing S1, before, during and after the occurrence of active whisking. Employing multi-electrode recordings in all layers of barrel cortex in urethane-anesthetized mice, we find layer-specific changes in multi-unit activity for principal and neighboring barrel columns. While whisker stimulation evoked similar early responses (0–50 ms post-stimulus) across development, the late response (50–150 ms post-stimulus) decreased in all layers with age. Furthermore, peak onset times and the duration of the late response decreased in all layers across age groups. Responses to paired-pulse stimulation showed increases in spiking precision and in paired-pulse ratios in all cortical layers during development. Sequential activation of two neighboring whiskers with varying stimulus intervals evoked distinct response profiles in the activated barrel columns, depending on the direction and temporal separation of the stimuli. In conclusion, our findings indicate that the temporal sharpening of sensory-evoked activity coincides with the onset of active whisking.

KEYWORDS

cerebral cortex, cortical layer, in vivo, network activity, sensory processing

Abbreviations: ANOVA, analysis of variance; COX, cytochrome-oxidase; CSD, current-source density; DiI, 1,1′-dioctadecyl-3,3,3′,3′-tetramethyl indocarbocyanine; fps, frame per sceond; i.p., intraperitoneal injection; ISIs, inter-stimulus intervals; L2/3, layer 2/3; L4, layer 4; L5, layer 5; L6, layer 6; LED, light-emitting diode; LFPs, local field potentials; MUA, multi-unit activity; NW, neighboring whisker; P, postnatal day; PPR, paired-pulse ratio; PSTH, peri-stimulus time histograms; PW, principal whisker; S1, primary somatosensory cortex; SD, standard deviation; TTL, transistor-transistor logic.

Alexander van der Bourg and Jenq-Wei Yang are considered as co-first authors.

Fritjof Helmchen and Heiko J. Luhmann are considered as co-senior authors.

Edited by John Foxe Reviewed by Yohei Okubo and Jerry Chen.

All peer review communications can be found with the online version of the article.

1 | INTRODUCTION

Rodent primary somatosensory cortex (S1) is an established model to study the sensory representation of tactile stimuli, structural and functional plasticity, perceptual decisionmaking, and development (Campagner, Evans, Loft, & Petersen, 2018; Feldmeyer et al., 2013). Whereas various aspects of single- and multi-whisker sensory-evoked activity have been studied in detail in adult rodent barrel cortex, relatively little is known about cortical processing of whisker-evoked responses in young animals and its maturation during development, especially at the onset of active whisking behavior around postnatal day (P) 14. In mice, active whisking fully matures during the first three postnatal weeks. Vibrissae movements transition from spontaneous unilateral muscle twitches of the whisker pad in the first week after birth to regular bilateral rhythmic sweeps at the end of the third postnatal week (Arakawa & Erzurumlu, 2015; Grant, Mitchinson, & Prescott, 2012; Tiriac, Uitermarkt, Fanning, Sokoloff, & Blumberg, 2012). During the same period, cortical connectivity undergoes major reorganization, including the maturation of connectivity between layer (L) 4 and L2/3 (Feldmeyer, Lübke, Silver, & Sakmann, 2002; Stern, Maravall, & Svoboda, 2001) and strengthening of local connectivity within L2/3 (Clem & Barth, 2006; Clem, Celikel, & Barth, 2008; Feldmeyer, Lübke, & Sakmann, 2006; Itami & Kimura, 2012; Wen & Barth, 2011). In parallel to the maturation of cortical connectivity, spontaneous activity transforms from highly correlated bursts of action potential firing (Khazipov & Luhmann, 2006; Yang, Hanganu-Opatz, Sun, & Luhmann, 2009) to desynchronized and sparse activity in the second postnatal week (Golshani et al., 2009; Luhmann & Khazipov, 2018). The functional maturation of barrel cortex circuitry is also reflected in layer-specific changes in sensory-evoked activity around P14, with increasing response selectivity to different stimuli and reduced adaptation (van der Bourg et al., 2017). Furthermore, increased lateral spread of responses to single-whisker deflections across neighboring barrel columns as well as enhanced communication with other sensory areas are observed at the onset of whisking behavior and considered to be essential for multisensory integration of tactile information (Ackman, Zeng, & Crair, 2014; van der Bourg et al., 2017; Quairiaux, Megevand, Kiss, & Michel, 2011).

Responses of individual barrel cortex neurons to isolated single-whisker stimulation are well studied (Brecht, Roth, & Sakmann, 2003; Hemelt, Kwegyir-Afful, Bruno, Simons, & Keller, 2010; Manns, Sakmann, & Brecht, 2004). However, during active tactile exploration rodents contact objects with multiple whiskers, resulting in complex and spatiotemporally diverse activation patterns (Wolfe et al., 2008). Neurons in S1 are highly sensitive to such stimuli and respond differentially to distinct directional force components exerted on the whisker upon touch as well as timing of touch events during active whisking (van der Bourg et al., 2017; Diamond, von Heimendahl, Knutsen, Kleinfeld, & Ahissar, 2008; Pammer et al., 2013). Previous studies using sequential stimulation of two neighboring whiskers (NW) with varying inter-stimulus intervals (ISIs) increased our understanding of the cortical signal processing to multi-whisker stimulation. Most of the studies found that deflection of the NW suppresses neuronal responses evoked by principal whisker (PW) deflection for up to 100 ms (Boloori, 2006; Erchova, Petersen, & Diamond, 2003; Higley & Contreras, 2005). Besides this suppression effect, other studies found facilitation of PW responses by preceding deflection of a NW within 10 ms (Ego-Stengel, Mello e Souza, Jacob, & Shulz, 2005; Kida, Shimegi, & Sato, 2005; Shimegi, Akasaki, Ichikawa, & Sato, 2000). These discrepancies possibly are due to differences in experimental procedures, e.g. the ISI range used or the different types of cortical layers and cells targeted by the specific electrophysiological techniques (Ego-Stengel et al., 2005).

Here, we applied a novel whisker stimulator (van der Bourg et al., 2017) to examine spatiotemporal processing of neuronal responses to single- and dual-whisker stimuli in developing mouse barrel cortex of three defined age groups (before, during, and after the emergence of active whisking). We recorded multi-unit activity (MUA) in anatomically well-defined locations and applied single- and dual-whisker stimuli in a systematic manner. Our experimental results reveal a substantial refinement of spatiotemporal processing of whisker-evoked activity in mouse barrel cortex around the onset of active whisking behavior.

2 | MATERIALS AND METHODS

2.1 | Animal surgery and preparation

All preparations and experiments were approved by the local German ethics committee (#23177-07/G10-1-010) and followed European and German regulations (European Communities Council Directive, 86/ 609/ECC). Electrophysiological experiments were conducted in 18 C7BL/6 mice (nine males and nine females) at ages ranging from P11 to P27. Mice were sedated with chlorprothixene (0.1 g/kg, intraperitoneal injection, i.p.; Sigma-Aldrich Chemie GmbH, Buchs, Switzerland) and anesthetized with urethane (0.25–0.5 g/kg, i.p.). Body temperature was maintained at 37°C with a heating pad. Hydration levels were checked regularly and maintained by subcutaneous injections of Ringer-lactate (Fresenius Freeflex; Fresenius Kabi AG, Oberdorf, Switzerland). Sufficient depth of anesthesia was evaluated regularly by testing absence of the hind paw pinch withdrawal reflex. Spontaneous whisker movements were not observed during anesthesia.

A custom-built head plate was glued to the skull with dental cement (Caulk Grip Cement) to secure and stabilize

the animal's head during electrophysiological recordings. After identifying the location of the C1 and C2 barrel columns through the skull using intrinsic optical imaging, a small cranial window of 1.5×1.5 mm^2 was opened with a sharp razor blade and superfused with Ringer's solution (in mM: 145 NaCl, 5.4 KCl, 10 HEPES, 1 $MgCl_2$, 1.8 $CaCl_2$; pH 7.2 adjusted with NaOH). The exposed neocortex was then penetrated by the multi-electrode array impregnated with DiI (1,1′-dioctadecyl-3,3,3′,3′-tetramethyl indocarbocyanine; Molecular Probes, Eugene, OR) and sealed with agarose (type III-a, 1% Ringer; Sigma).

2.2 | Galvanometer-driven whisker stimulation

Whisker stimulation was performed with two galvanometer-driven stimulation system using optical fibers attached to individual whiskers as described previously (van der Bourg et al., 2017). One stimulation fiber was attached to each the C1 and C2 whisker, respectively, considering variations in resting position angles and relative anterior-posterior shifts. The stimulation fibers were fixed and secured with Plasticine on top of a custom-built holder plate and secured and translated with a micro-manipulator. Deflections were applied in the rostrocaudal direction with varying amplitudes and ISIs. The individual stimulation pulses consisted of a 100-Hz phase-shifted cosine wave with varying peak velocities.

2.3 | Intrinsic optical imaging

The C1 and C2 barrel columns were identified using optical imaging of intrinsic signals. Reference images of the cortical blood vessel pattern were visualized by a 546-nm LED to enhance contrast. Functional maps of the targeted barrel columns were obtained by shining red light (625 nm LED) on the cortical surface while stimulating the C1 or C2 whiskers individually. A single whisker was deflected with a protruding device consisting of a miniature solenoid actuator which was controlled by a transistor-transistor logic pulse. The actuator tip was placed orthogonal to the base of the whisker around 2 mm from the snout. Whiskers were stimulated rostro-caudally with peak velocity of 1,140°/s. Stimuli were presented for 5 s at 5 Hz with 8 s ISIs. Reflectance images were collected with a MiCam ultima L high-speed camera system (Scimedia, Costa Mesa, CA; 100×100 binned pixels, for 100 μm per pixel). Using a C-mount extension tube, the field of view was limited to 2.6×2.6 mm^2 to reduce vignetting (26 μm pixel size, 500 fps). Functional intrinsic signal images were computed as fractional reflectance changes relative to the pre-stimulus average across 10 trials. The intrinsic signal images obtained for the C1 and C2 barrel columns were then mapped to the blood vessel pattern to guide the location of the craniotomy and insertion of the multi-electrodes.

2.4 | High-density multi-electrode recordings in vivo

Neural activity was recorded with a 4-shank 80-channel silicon probe (NeuroNexus Technologies, Ann Arbor, MI) inserted perpendicular into the C1 and C2 columns of barrel cortex. Each of the four shanks (length 3 mm) contained 20 recording sites spaced 50 μm apart. The distance between shanks was 150 μm. Insertion of the probe was guided by intrinsic optical imaging. Before insertion, the probe was impregnated with the DiI (1,1′-dioctade- cyl-3,3,3′3′-tetramethylindocarbocyanine; Molecular Probes, Eugene, OR) which was dissolved in 70% ethanol. The tracks of the four shanks were identified by the DiI fluorescence. All data were continuously digitized at 20 kHz and stored offline on a 256-channel extracellular recording system running MC_Rack software (Multi Channel Systems, Reutlingen, Germany).

2.5 | Histology

After each experiment, the animal was deeply anesthetized with ketamine (120 mg/kg, ketamine, 50 mg/ml; Hameln Pharma, Hameln Germany) and xylazine (5 mg/kg, Rompun 2%; Bayer, Leverkusen, Germany) and perfused through the aorta with 0.2 M phosphate-buffered saline. The brain was post-fixed in 4% paraformaldehyde as described in detail previously (van der Bourg et al., 2017). The brains were sectioned tangentially (200 μm thickness). First, we checked the DiI fluorescence to identify the tracks of the four shank probe; subsequently, brain slices were stained with cytochrome-oxidase (COX) to identify the barrel map. Combining the DiI fluorescence with the COX-barrel map, we could verify the location of the electrodes in C1 or C2 barrels.

2.6 | Analysis of current-source density maps

Current-source density (CSD) maps were computed as the second spatial derivative from the average local field potentials (LFPs) of up to 100 trials as described previously (Mitzdorf, 1985; Nicholson & Freeman, 1975; Reyes-Puerta, Sun, Kim, Kilb, & Luhmann, 2015). The computed data were interpolated and visualized as pseudo-color images with current sources and sinks represented by red (positive) and blue (negative) colors respectively. Early CSD sinks expected for the thalamo-recipient L4, L5, and L6 (Figure 1b,c) were used to assign recording sites to cortical layers (Reyes-Puerta et al., 2015).

2.7 | Analysis of evoked MUA

Data were imported and analyzed offline using MATLAB (v7.7; Mathworks, Natick, MA). The continuously recorded raw data signals were high-pass filtered (0.8–5 kHz) and MUA was

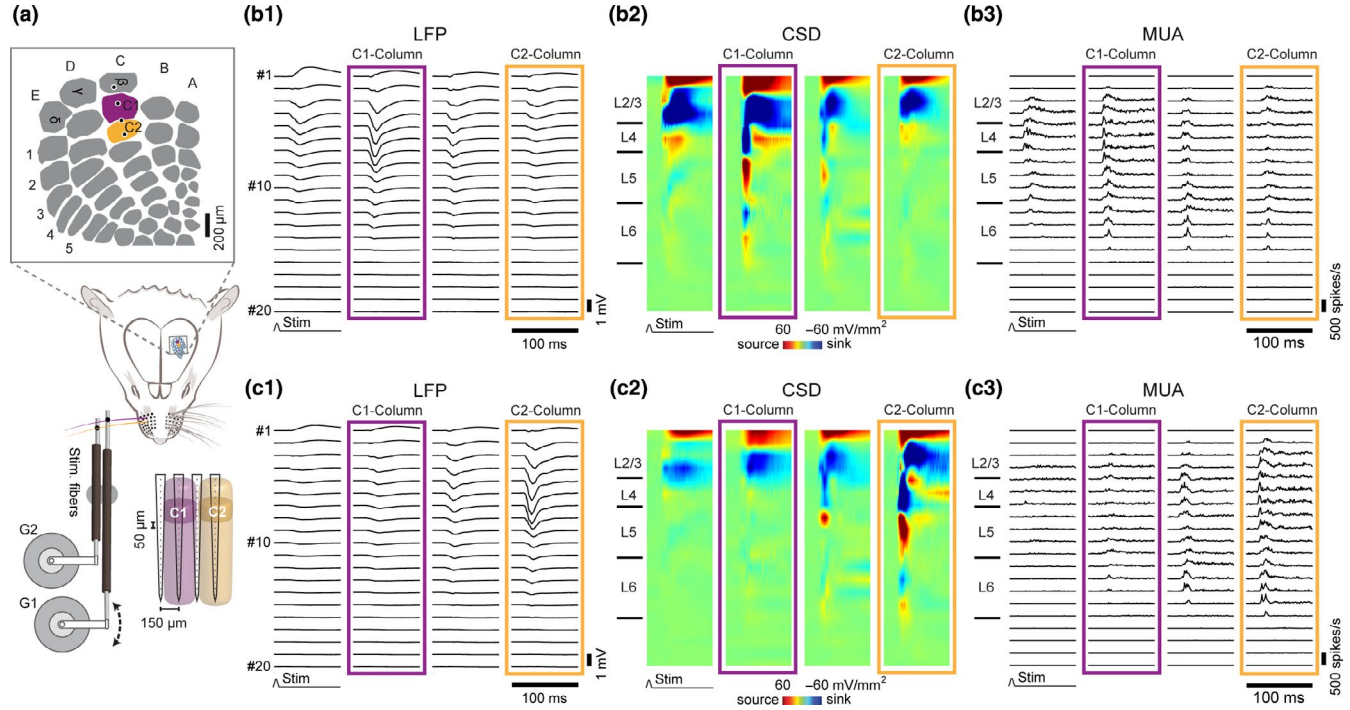

FIGURE 1 Multi-electrode array recordings of neuronal activity in C1 and C2 barrel-related columns following stimulation of whisker C1 (b) or C2 (c). (a) Schematic diagram of multi-electrode array placement in a schematic top view of the barrel field (top) and the stimulation of the C1 or C2 whiskers using galvanometer-driven stimulation system 1 and 2 (G1 and G2, bottom). (b) Example neuronal responses to C1 whisker stimulation in a P13 mouse. Representative local field potential (LFP, (b1) recordings across layers and their corresponding current-source density (CSD, (b2) maps computed from 100 stimulation pulses applied to the C1 whisker (half-cosine pulse, 10 ms pulse-width, 1,140°/s peak velocity). CSD sinks are indicated by blue and sources by red colors. The corresponding evoked multi-unit activity (MUA, (b3) on all channels for the same single-whisker stimulation. The borders between cortical layers were identified from the CSD maps. (c) Same as in b but for stimulation of the C2 whisker. [Colour figure can be viewed at wileyonlinelibrary.com]

extracted by applying a threshold at 7.5 times the standard deviation of the baseline (*SD*). According to the onset of stimuli, the peri-stimulus time histograms were calculated with a resolution of 1 ms bin and then smoothed by 5 ms sliding window averaging. The peak of evoked MUA firing rate and the mean MUA firing rate in this study were calculated with subtraction of the baseline mean firing rate (before stimulus onset time 100 ms).

2.8 | Effect size calculation

We calculated the η^2 to evaluate the effect size of stimulus velocities, ages, and their interaction on the evoked MUA using the mes2way function in the MES toolbox (Hentschke & Stüttgen, 2011). The η^2 was calculated as

$$\eta^2 = \frac{SS_{effect}}{SS_{total}}$$

where SS_{effect} denotes the sums of squares for the effect of interest and SS_{total} denotes the total sums of squares for all effects, interactions, and errors in the ANOVA.

2.9 | Statistical analysis

The majority of data were represented as box plots, in which the central line marks the median, the edges represent the 25th and 75th percentiles, the whiskers extend to the most extreme data points, and outliers are plotted individually. We performed D'Agostino & Pearson omnibus normality tests to test for normal distribution of the data. Paired *t*-test, and one- or two-way ANOVA were used to test for significance for normally distributed data, followed by post-hoc Tukey's multiple comparison test. The Wilcoxon signed-rank test or Kruskal–Wallis test were used for non-normally distributed data, followed by Dunn–Sidak's post-hoc multiple comparison test. The significance threshold was set to $p < 0.05$; in the figures, different degrees of evidence against the null hypothesis are indicated by asterisks ($*p < 0.05$; $**p < 0.01$; $***p < 0.001$).

3 | RESULTS

3.1 | Measuring neuronal activity in developing barrel cortex with silicon probes

We recorded neuronal activity by inserting silicon-probes into barrel cortex of urethane-anesthetized mice in three different age groups: before eye opening and whisking onset (P11–12), during the critical period (P13–15) and afterwards (P23–27) (Figure 1a). We measured LFPs and MUA simultaneously across all layers of the C1 and C2 barrel columns

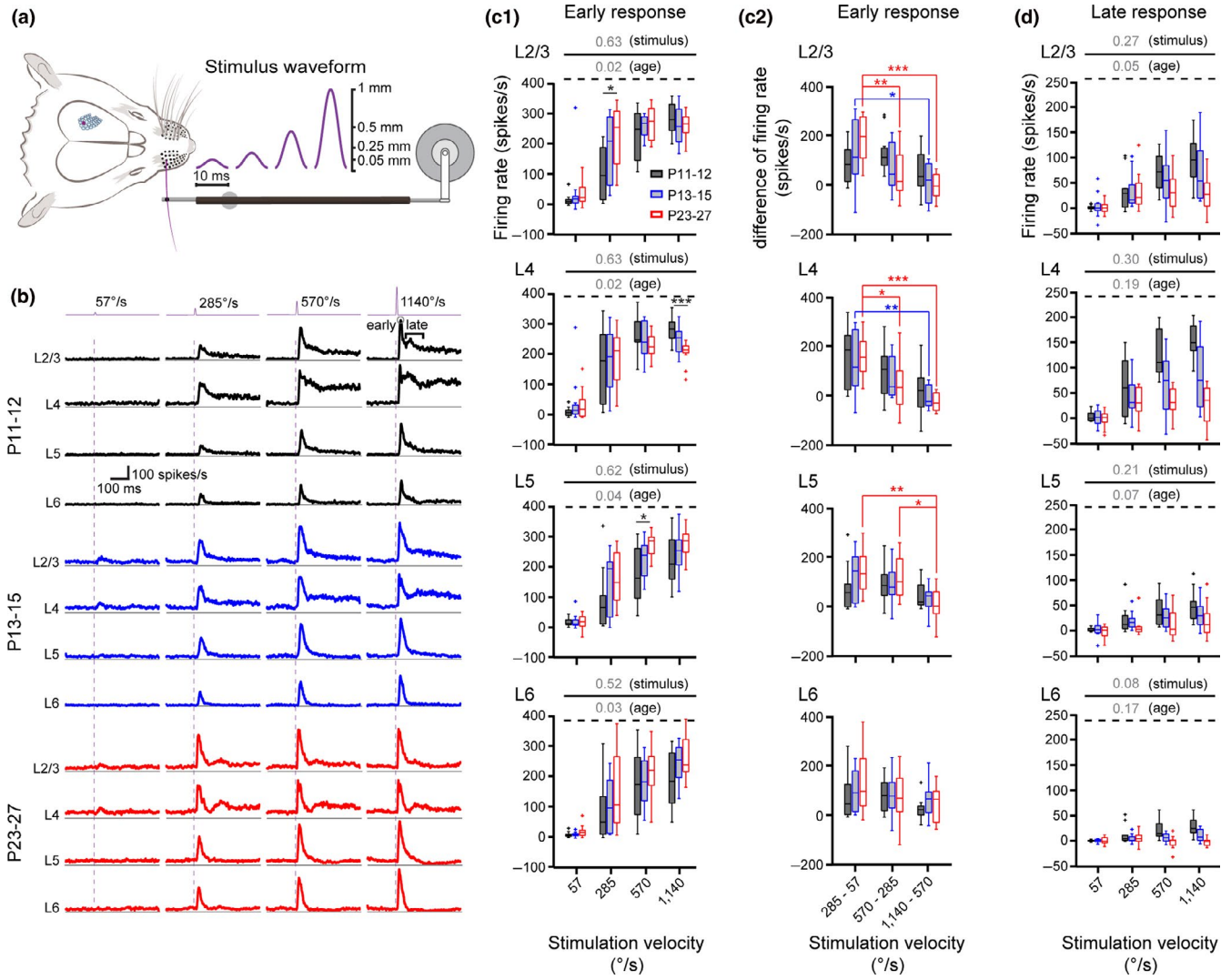

FIGURE 2 Age-dependent changes in evoked multi-unit activity (MUA) following single-whisker stimulation with different stimulus velocities. (a) Schematic diagram of single-whisker stimulation with different stimulus velocities (10 ms half-cosine pulses with peak velocities ranging from 57°/s to 1,140°/s). (b) Average of evoked MUA in different cortical layers from three age groups induced by different stimulus velocities. For each animal, after identifying the cortical layers according to the evoked current-source density map (Figure 1), we separately selected four electrodes corresponding to the centers of L2/3, L4, L5, and L6 for the analysis. (c) Quantification of the peak amplitude of the early response (0–50 ms after stimulus onset) for all stimulus velocities and layers (c1), and the difference of MUA firing rates between different stimulus velocities (c2). (d) Quantification of the mean firing rate in the late response window (50–150 ms after stimulus onset) for all stimulus velocities and layers. Data points are mean ± *SEM* ($n = 12$ recordings from six mice per age group). Note: number (gray color) in c1 and d show η^2 values to indicate effect sizes of stimulus velocities and ages. The repeated measures ANOVA were used in c2 followed by post-hoc Tukey's multiple comparison test. [Colour figure can be viewed at wileyonlinelibrary.com]

(Figure 1b,c) while stimulating one or two whiskers with high temporal and spatial precision using a galvanometer-driven whisker stimulator (van der Bourg et al., 2017). Our stimulation protocol consisted of single-whisker stimulation with different stimulus velocities (Figure 2a), single-whisker paired-pulse stimulation with varying ISIs (Figure 4a), and dual-whisker stimulation where the C1 and C2 whiskers were deflected sequentially with varying ISIs (Figure 6a). These specific stimulus sets allowed us to study the neural representation of spatiotemporally distinct stimuli in developing mouse barrel cortex.

3.2 | Layer-specific modulation of sensory-evoked responses by varying stimulus velocity

First, we asked how neurons in different layers and age groups encode single-whisker deflections with different stimulus velocities (Figure 2a). At all age groups, MUA in L2/3 and L4 evoked by single-whisker stimulation at high stimulus velocity (1,140°/s) displayed a fast component followed by a slow component (Figure 2b). Therefore, we analyzed MUA across all layers and age groups by subdividing the response into an "early" (0–50 ms) and "late" (50–150 ms)

component (Figure 2c,d). We found that low-velocity whisker deflections (<60°/s) resulted in barely detectable sensory-evoked responses, comparable to spontaneous activity (<50 spikes per s) in all layers. Higher stimulus velocities resulted in increasingly higher spike rates across all layers (Figure 2b). Interestingly, the increase in spike rate displayed a layer-specific and age-dependent response profile differently for the early and late response. For the early response, MUA firing rates in all layers increased significantly with increasing stimulus velocities ($\eta^2 > 0.5$), but the curves of MUA firing rate were similar across age groups ($\eta^2 < 0.05$) (Figure 2c1). In addition, at a stimulus velocity

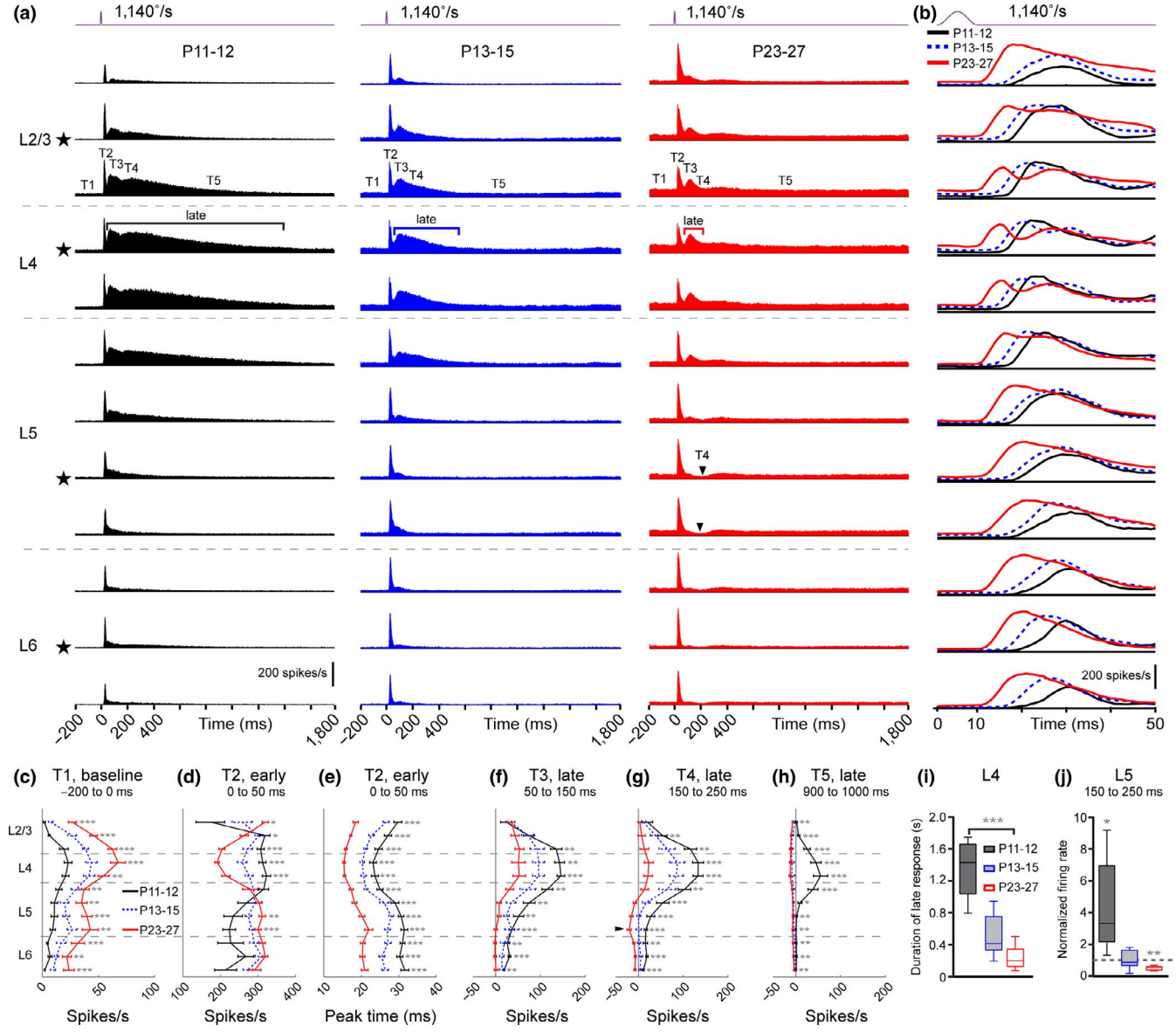

FIGURE 3 Temporal refinement of sensory-evoked multi-unit activity (MUA) after single-whisker deflection at 1,140°/s. (a) Mean evoked MUA after single-whisker deflection in different cortical layers and age groups ($n = 8$ recordings from four mice for P11–12 and P13–15 age groups; $n = 10$ recordings from five mice for P23–27 age group). T1: −200 ms to 0 ms before stimulus onset. T2: 0–50 ms; T3: 50–150 ms; T4: 150–250 ms; T5: 900–1,000 ms after stimulus onset. In the upper channel of L4, late responses are marked. Arrowheads in L5 for the P23–27 age group indicate transient inhibition of the MUA responses. (b) Superimposed mean evoked MUA at 0–50 ms post-stimulus in the three age groups. Same data as in (a), but on expanded time scale. (c) Mean baseline firing rates (−200 to 0 ms before stimulus onset) in different cortical layers and age groups. (d) MUA firing rate of early responses. (e) Peak time of early responses. (f) Mean MUA firing rate during 50–150 ms after stimulus onset. (g) Mean MUA firing rate during 150–250 ms after stimulus onset. Note: negative MUA firing rate in deeper L5 (black arrowhead as indicated in panel a) for the P23–27 age group. (h) Mean MUA firing rate during 900–1,000 ms after stimulus onset. (i) Duration of late response activity in L4 (from the end of early response to the time point when MUA activity declined below the onefold standard deviation of the baseline, see panel a). (j) Comparison of mean firing rate at 150–200 ms in L5 of the three age groups. Statistics: Kruskal–Wallis test for panel c–h, Kruskal–Wallis test followed by Dunn–idak's post hoc multiple comparison test for panel i, and Wilcoxon matched-pairs signed rank test to compared with value 1 for panel j. [Colour figure can be viewed at wileyonlinelibrary.com]

of 285°/s the MUA firing rate in L2/3 was significantly higher in the P23–27 than P11–12 age group. Furthermore, analyzing the difference of MUA firing rates between different stimulus velocities, we found that in L2/3 and L4, the evoked MUA of the P13–15 and P23–27 age groups reached a plateau already at a stimulus velocity of 570°/s, which in L5 was the case only for the P23–27 age group (Figure 2c2). These results demonstrate that the whisker-to-barrel cortex system increases its sensitivity to single whisker deflection during early development. For the late response, we found a similar dependence of MUA mean firing rate on stimulus velocities in L2/3, L4 and L5 ($0.21 < \eta^2 < 0.3$; all significant), but not for L6 ($\eta^2 = 0.08$) (Figure 2d). However, in stark contrast with the minor differences between age groups for the early response ($\eta^2 < 0.04$), we found a significant reduction in late response MUA with age in all layers, most notably in L4 and L6 (significant main or interaction effects, or both; $0.05 < \eta^2 < 0.19$).

3.3 | Maturation of temporal processing of whisker-evoked responses

Next, we investigated how sensory information is processed across cortical layers using our strongest single whisker deflection (1,140°/s) because this stimulation induced the most robust response in all cortical layers and age groups (Figure 3). Several changes in MUA were observed during development (Figure 3a,b). First, baseline firing rate

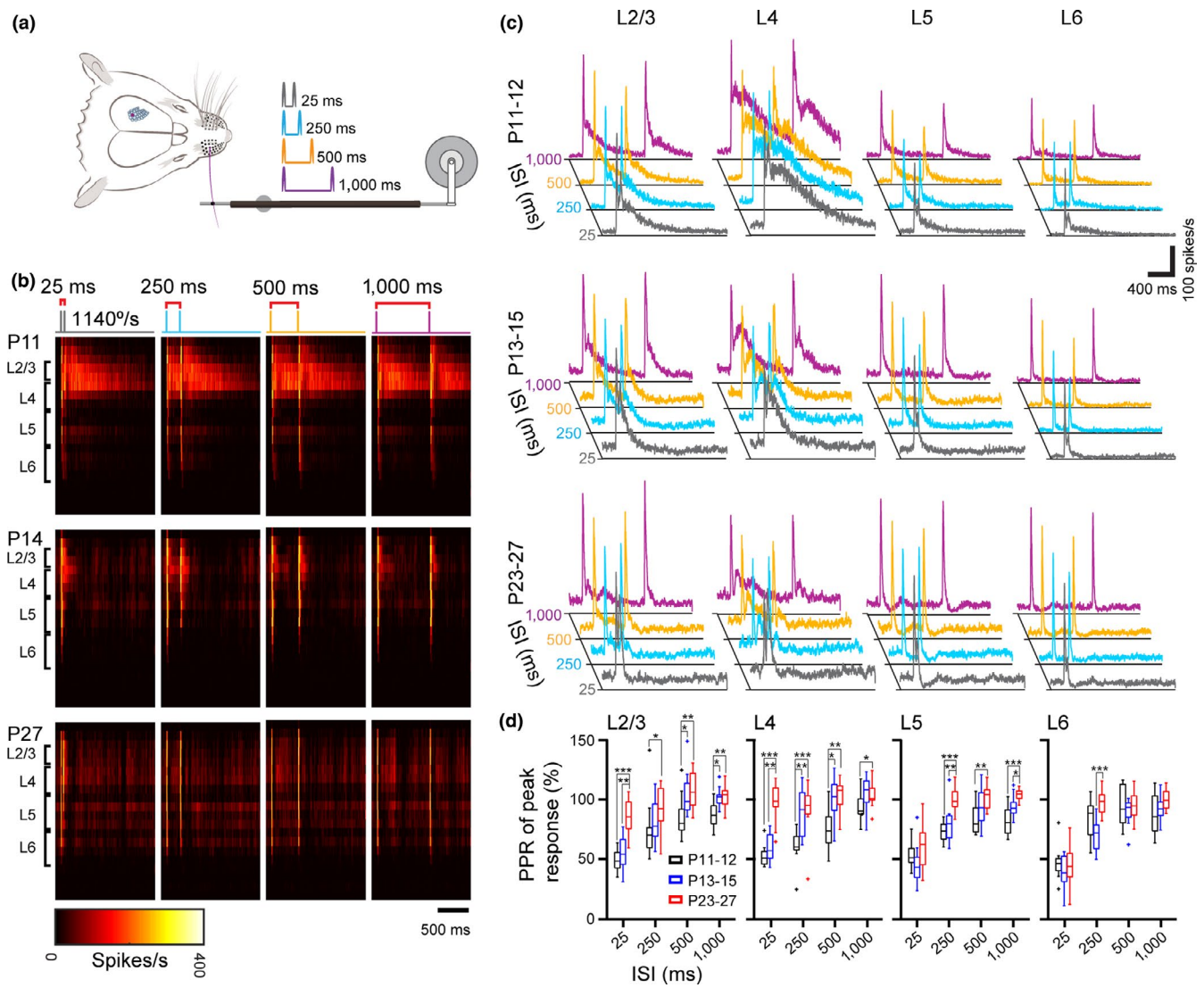

FIGURE 4 Sensory-evoked multi-unit activity (MUA) activity after paired-pulse stimulation with different inter-stimulus intervals (ISIs). (a) Schematic illustration of paired-pulse single-whisker stimulation with 1,140°/s stimulus velocity and ISIs ranging from 25 to 1,000 ms. (b) Heatmaps of MUA in the principal whisker-related barrel column (c1) after paired-pulse single whisker deflections with different ISIs. Examples from individual mice aged P11, P14, and P27 respectively. (c) Average MUA following paired-pulse stimulation with different ISIs for the three age groups. (d) Average paired-pulse ratio (PPR, second vs. first) of peak responses in different layers for the three age groups ($n = 12$ recordings from six mice per age group). Statistics: Kruskal–Wallis test followed by Dunn–Sidak's post hoc multiple comparison test. [Colour figure can be viewed at wileyonlinelibrary.com]

increased significantly across all cortical layers between the P11–12 and P23–27 age groups (Figure 3a,c). Second, the peak firing rate of the early responses decreased significantly in deep L2/3 and L4, but increased significantly in deep L5 during development (Figure 3b,d). Third, the peak latency of the early response decreased significantly across all cortical layers between P11–12 and P23–27 (Figure 3b,e). Fourth, in the P11–12 age group, we observed a strong and persistent late response lasting several hundreds of milliseconds, especially in L4 and, to a lesser extent, ranging from deep L2/3 to upper L5 (Figure 3a). The strength and duration of this late response gradually declined at P13–15 and P23–27, demonstrating a developmental refinement of sensory-evoked activity after single-whisker deflection (Figure 3f–i). Finally, we could also detect a significant inhibition in MUA activity around 150–250 ms after stimulus onset in deep L5 in the P23–27 age group (Figure 3a, g and j). The developmental temporal refinement of sensory-evoked activity was also significantly for 570°/s whisker deflection and the same trend was additionally observed for 285°/s whisker deflection, albeit not reaching significance (Figures S1 and S2).

3.4 | Temporal sharpening of MUA evoked by paired-pulse single whisker deflections

Next, we studied how paired-pulse single whisker deflections with a wide range of ISIs (25–1,000 ms) are processed in different cortical layers (Figure 4). We found that the paired-pulse ratio (PPR) of the early peak responses revealed layer-specific changes across development (Figure 4b–d). In all three age groups and in all layers, the second response for 1,000 ms ISI was minimally reduced compared to the first response except for L5, which displayed ~30% reduction in the second versus first peak-response in the P11–12 age group (Figure 4c,d). For 250 and 500 ms ISIs, a significant reduction in the second response compared to the first response was observed at P11–12 and P13–15, but not at P23–27. For 25 ms ISI, the second response were strongly reduced in all layers of the P11–12 and P13–15 age groups, whereas at P23–27 similar reductions were found only in L5 and L6 but not in L2/3 and L4 (Figure 4c,d). These results demonstrate that during development the temporal precision and discriminability of MUA responses evoked by repetitive whisker stimulation increases at short ISI (25 ms), especially in L2/3 and L4.

3.5 | Cross-columnar spread of early responses increases during development

Next, we addressed the question how single-whisker deflection evoked activity propagates to neighboring cortical columns (Figure 5a). Consistent with our previous study, in which we applied repetitive single whisker stimuli (van der Bourg et al., 2017), we found increased cross-columnar

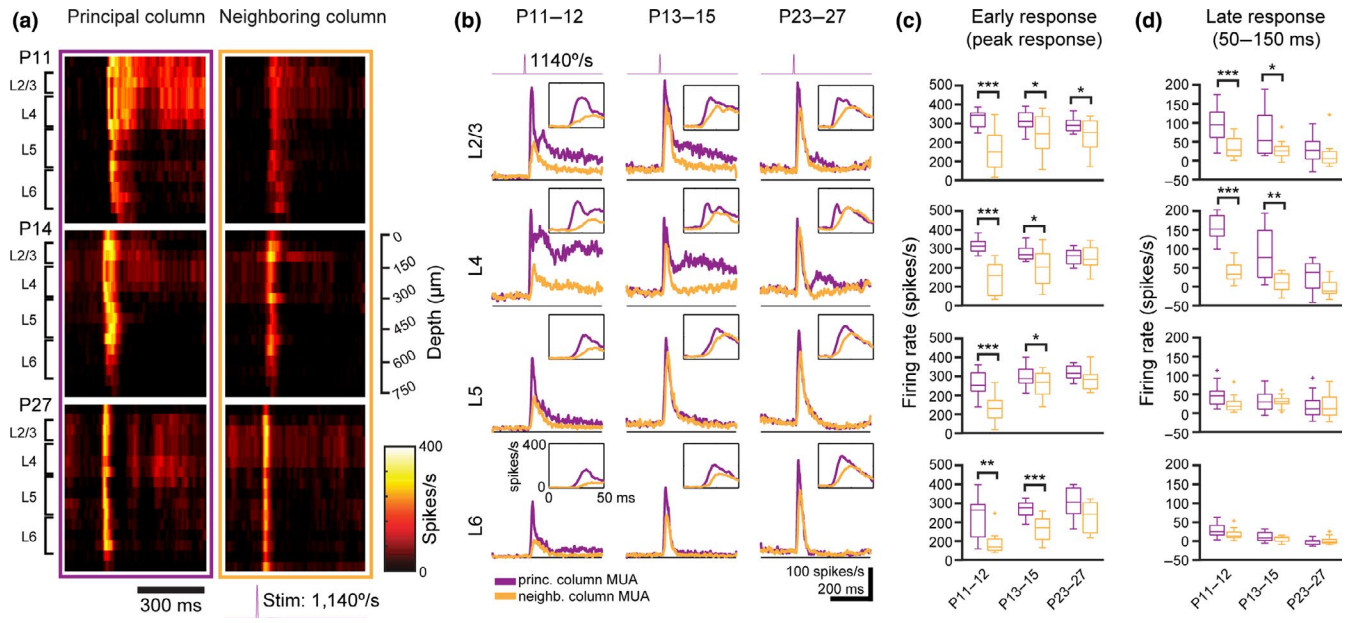

FIGURE 5 Changes in cross-columnar spread during development. (a) Heatmap showing multi-unit activity (MUA) for the first 500 ms in the principal (C1) and neighboring (C2) barrel column after single-whisker deflection (1,140°/s). Examples from recordings of individual mice aged P11, P14, and P27 respectively. (b) Average MUA in different layers of principal (purple) and neighboring (orange) barrel column for all mice ($n = 12$ recordings from six mice per age group). Note: inset shows the MUA peak delay of early response (0–50 ms) in neighboring barrel column than principal barrel column. (c) Analysis of peak MUA for the early response (0–50 ms) in different layers of the principal (purple color) and neighboring (orange color) barrel column for all mice. (d) Analysis of the mean MUA for the late response (50–150 ms) in different layers of the principal (purple color) and neighboring (orange color) barrel column for all mice. Statistics: paired *t*-test. [Colour figure can be viewed at wileyonlinelibrary.com]

spread of activity with development (Figure 5b). At P11–12 and P13–15, the early MUAs in the neighboring barrel column were significantly smaller in all layers than in the principal column (Figure 5c). However, this difference was almost completely absent at P23–27, which was mostly due to an increase in response strength in the neighboring barrel column (rather than a decrease in the principal column). Although the amplitude of the MUA response in the neighboring barrel column reached the same level of the principal barrel column at P23–27, there is a clear peak time delay of the evoked MUA in neighboring than principal barrel column (Figure 5b, insets; $p < 0.001$ in L2/3, L4 and L6; $p < 0.05$ in L5; $n = 12$ both for principal and neighboring barrel column, paired-t test). In contrast with the early response, we observed a developmental decline in the late response strength both in principal and neighboring barrel columns especially in L2/3 and L4 (Figure 5d).

3.6 | Sequential dual-whisker stimulation elicits distinct barrel-specific activity profiles

As outlined in the Introduction, exploratory locomotion is characterized by complex spatiotemporal stimulation profiles of the entire whisker array. To investigate the developmental trajectory of spatiotemporal processing in a controlled manner, we sequentially stimulated the PW and the NW with varying ISIs, with PW deflection either preceeding or following NW deflection (Figure 6a). As expected, these different PW–NW stimulation sequences resulted in differential activation profiles (Figure 6b and Figures S3–S5). Stimulating the NW first resulted in unchanged or only slightly reduced PW-evoked MUA responses in L2/3 and L4 of the principal column across all age groups and regardless of ISI. However, in L5 and L6 we observed a moderate (P11–12) to strong (P13–15, P23–27) reduction in PW-responses, especially with 50 ms ISI (Figure 6c; NW→PW, purple traces). When deflecting the PW first, NW-evoked responses were generally small and could only be clearly discerned at ISIs of 50 and 100 ms. We observed a developmental reduction in the ratio of NW-evoked peak responses by deflecting the PW prior at 50 ms but not at 100 ms ISI (Figure 6c; PW→NW, orange traces; Figure 6d). These results suggest an increase in the strength of cortico-cortical connectivity and imply an increased center-surround suppression of sensory-evoked activity.

4 | DISCUSSION

We have characterized the developmental profile of whisker-evoked responses in mouse barrel cortex between P11 and P27. The main findings of the present study are the following: (a) Single-whisker deflections evoked similar early responses in all layers and all age groups. The long-lasting elevated firing rate in the late response was most prominent in L4 and decreased during development. (b) During development the latency of the early responses and the duration of the late responses to high and medium velocity stimulation decreased. (c) Paired-pulse whisker stimulation revealed a layer-specific suppression of the response to the second stimulus, which was most pronounced in younger animals and at short ISIs (25 ms). (d) The trans-columnar spread of early activity increased during development. (e) Sequential activation of two NW at varying ISIs revealed a strong suppression of the second response, which was most pronounced in >P13 animals. In summary, our data demonstrate a developmental sharpening in the temporal processing of whisker-evoked activity around and after the onset of active whisking behavior which is in-line with the previous findings in visual and barrel cortex (Colonnese et al., 2010; Minlebaev, Colonnese, Tsintsadze, Sirota, & Khazipov, 2011).

4.1 | Developmental changes of single-whisker evoked activity

Spontaneous baseline firing rate gradually increased with development in all cortical layers and was highest in all age groups in L4 (Figure 3c). The distribution of spontaneous firing rate across layers was correlated with the distribution of cell density in cortical layers of barrel cortex, especially, highest in L4 (Meyer et al., 2013). Because the cortical neuronal density and the thickness of cortical layers do not change substantially from P11 to P27 (Chang, Suzuki, & Kawai, 2018), the comparisons of amplitudes of evoked MUA across development in this study are not strongly influenced (biased) by the change of cortical neuronal density during development. A large number of previous studies in adult barrel cortex have demonstrated that neurons are highly sensitive to velocity and acceleration of whisker stimulation with spikes rates increasing at higher stimulus velocities (Lee & Simons, 2004; Wilent & Contreras, 2004). Our results corroborate these previous findings in adult rodents and further show that neurons in all layers increase their sensory-evoked spiking rates with increasing stimulus velocity across all age groups (Figures 2 and 3). Interestingly high firing rates in the early response could be already observed in L2/3 and L4 of P11–12 animals (Figure 2c), demonstrating that the sensory input strongly activates these layers at surprisingly early developmental stages. In all layers the latency of the first response (Figure 3b) became progressively shorter with development, reflecting the maturation of synaptic connections in the whisker-to-barrel cortex pathway (Feldmeyer et al., 2013). Another important finding of our study is the pronounced late MUA response in the younger age groups, which as the early response was strongest in L2/3 and L4 (Figures 2d and 3f–i). This late evoked response progressively decreased during

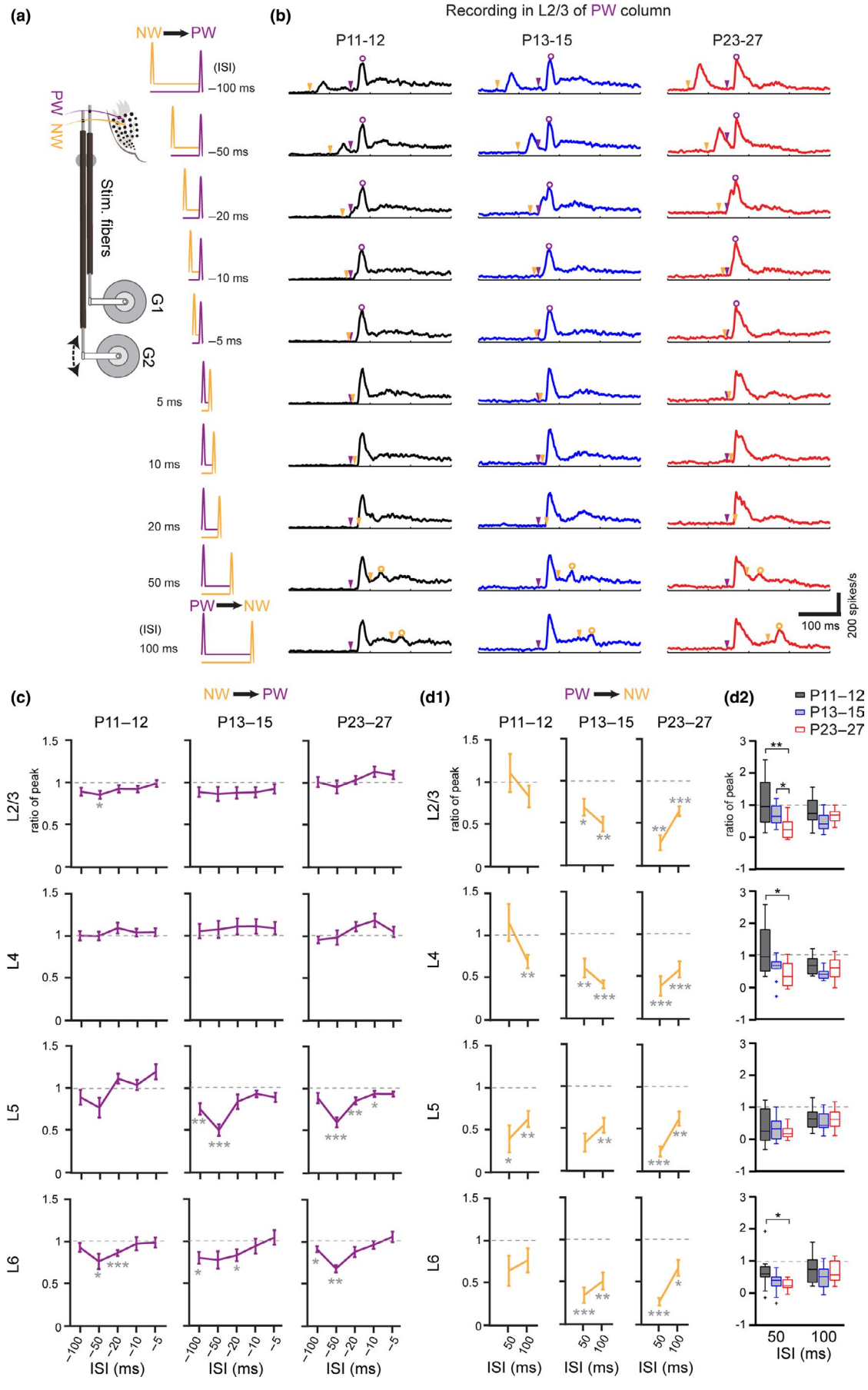
(a)
NW → PW
(ISI)
–100 ms
–50 ms
–20 ms
–10 ms
–5 ms
5 ms
10 ms
20 ms
50 ms
PW → NW
(ISI)
100 ms
PW
NW
Stim. fibers
G1
G2
(b)
Recording in L2/3 of PW column
P11-12
P13-15
P23-27
100 ms
200 spikes/s
(c)
NW → PW
P11–12
P13–15
P23–27
L2/3
L4
L5
L6
ratio of peak
ISI (ms)
(d1)
PW → NW
(d2)
P11–12
P13–15
P23–27
50
100

FIGURE 6 Multi-unit activity (MUA) activity after sequential deflection of the principal whisker (PW) and the neighboring whisker (NW). (a) Schematic illustration of the stimulation paradigm. Whiskers were either sequentially activated by deflecting the NW first followed by PW stimulation (NW→PW) or by deflecting the PW first followed by NW stimulation (PW→NW). ISIs varied between 5 and 100 ms. (b) Mean evoked MUA in L2/3 of principal barrel column following the set of different dual-whisker stimulation sequences ($n = 12$ recordings from six mice per age group). Gray arrowheads indicate onsets of NW stimulation; black arrowheads indicate onsets of PW stimulation. Black and gray circles indicate the peak MUA following PW and NW stimulation, respectively. Note clear MUA peaks following NW stimulation for ISIs of −100 ms, −50 ms, 50 ms and 100 ms. (c) MUA when NW is stimulated prior to PW. Average ratio of peak response to PW stimulation at −5, −10, −20, −50, and −100 ms ISIs (black circles in b) to peak response at 100 ms ISI (lower trace in b). Statistics: Wilcoxon signed-rank test. (d1) MUA when PW is stimulated prior to NW at 50 and 100 ms ISI. Average ratio of peak response to NW stimulation at 50 and 100 ms ISI (gray circles in b) to peak response at −100 ms ISI (upper trace in b). Statistics: Wilcoxon signed-rank test. (d2) Analysis of the ratio of peak response for NW stimulation at 50 and 100 ms conditions of all layers and all age groups. The ratios of peak response were calculated as the peak of MUA evoked by NW stimulation in 50 or 100 ms ISI conditions compared to −100 ms ISI. Statistics: Kruskal–Wallis test followed by Dunn–Sidak's post hoc multiple comparison test. [Colour figure can be viewed at wileyonlinelibrary.com]

further development and was weak or absent in infragranular layers. This developmental change presumably is governed by maturation of local connectivity, including changes in synapse density (Chandrasekaran et al., 2015) and local connectivity between L4-to-L2/3 and L2/3-to-L2/3 neurons (Stern et al., 2001; Wen & Barth, 2011). Another explanation for this developmental reduction in the late response may be the maturation of the inhibitory network (Shoykhet, Land, & Simons, 2005), which is supported by our finding of clear inhibition of MUA in deep L5 emerging in the P23–27 age group (Figure 3g,j). This hypothesis is supported by the developmental maturation of GABAergic inhibition in rodent neocortex (Luhmann & Prince, 1991). Further plausible causes could involve the development of layer-specific densities in GABAergic interneurons in barrel cortex (Lefort, Tomm, Floyd Sarria, & Petersen, 2009; Meyer et al., 2011).

4.2 | Possible effects of urethane anesthesia on the evoked MUA activity

Urethane has been widely used in in vivo experiments as anesthetics due to its long-lasting effect and minimal impact on cardiovascular and respiratory function (Maggi & Meli, 1986). However, various effects on neurotransmitter-gated ion channels have been reported. For example, urethane potentiates nicotinic acetylcholine, $GABA_A$, and glycine receptors, whereas it inhibits NMDA and AMPA glutamate receptors (Hara & Harris, 2002). Urethane also changes sensory-evoked responses in visual, auditory, and somatosensory cortex in a dose-dependent manner (Capsius & Leppelsack, 1996; Devonshire, Grandy, Dommett, & Greenfield, 2010; Durand et al., 2016; Peng, Zhou, Shi, Hua, & Hua, 2011; Simons, Carvell, Hershey, & Bryant, 1992). In barrel cortex, Simons et al. (1992) reported that the early component of single-whisker evoked MUA was only slightly reduced, indicating that our analysis of early response components should be little affected by anesthesia. However, their study also found that the late component of evoked MUA was strongly enhanced under 1.5 g/kg urethane anesthesia when compared with the awake condition. In particular, the late component of MUA evoked by NW stimulation was strongly increased under urethane anesthesia (Simons et al., 1992). In order to reduce such an urethane effect on evoked MUA in our current study we first sedated mice with chlorprothixene and then applied lower doses of urethane (0.25–0.5 g/kg, i.p.) compared to previous studies (typically 1.5 g/kg; Durand et al., 2016; Pagliardini et al., 2013). In contrast with the observations by Simons et al. (1992), NW stimulation in our study did not evoke strong late MUA components in P23–27 age group (Figure 5). This suggests that the influence of urethane on evoked MUA was not as strong in our study. Our finding that the late-component response duration shortens during development is also unlikely to be due to an urethane effect because a similar observation has been reported in the visual cortex of awake mice (Shen & Colonnese, 2016). Nonetheless, it will be important and interesting to investigate the developmental profile of whisker-evoked cortical activity under more naturalistic and awake conditions.

4.3 | Developmental profiles of paired-pulse stimulation evoked MUA

Paired-pulse stimulation is commonly used to study the temporal properties of neuronal excitability (David-Jürgens & Dinse, 2010). Previously, a strong suppression of the response to the second stimulation has been shown in P7 mice even at long ISIs up to 5 s (Zehendner, Tsohataridis, Luhmann, & Yang, 2013). Here, we extended the investigation of developmental changes in PPR to the period between P11 and P27. The low PPR from 25 to 1,000 ms ISI in the P11–12 group (Figure 4) may be due to the high MUA firing rate of the late response to the first single whisker deflection, which can persist for more than a second (Figures 2 and 3). This reverberating activity may interfere with a re-activation of the MUA by the second whisker deflection. At P23–27 this mechanism is weaker because at this age the late response is shorter (~200 ms) and MUA firing rates are lower. Thus, at P23–27 PPR is near 100% for all ISIs. Our data demonstrate a gradual reduction in paired-pulse suppression during development, suggesting that mice gradually develop the ability to distinguish two successive stimuli more precisely, even at short ISIs of 25 ms.

4.4 | Cross-columnar spread of evoked activity

Analyzing the early response to single whisker stimulation in combined VSDI and multi-electrode LFP recordings, we could previously demonstrate in P0–P1 rat barrel cortex a functional topographic map as early as P0. At this age, the early response consisted of a gamma burst restricted to a local area of ~400 μm in diameter and the late response of a spindle burst activity covering a larger area of ~600 μm (Yang et al., 2013). Until P5 the evoked response was localized and starting from P6–P7, it spread to neighboring barrel-related columns (Yang et al., 2013). The area of the evoked response increased during further development from P7 to P21 (Borgdorff, Poulet, & Petersen, 2007). In the present study we show that already at P11, the early response in all layers spread to the neighboring column (Figure 5a–c). The activity in the neighboring column became larger with increasing age from P11 to P27, demonstrating the development of cross-columnar processing and multi-whisker receptive fields as reported previously (van der Bourg et al., 2017). This age-dependent increase in the area of evoked responses and cross-columnar activity spread is correlated with the structural development of neuronal connections within and between barrel-related columns. The thalamocortical inputs to L4 neurons are established during the first postnatal week when the dendritic arborizations of L4 neurons develop within their own barrel column (Espinosa, Wheeler, Tsien, & Luo, 2009). After the first postnatal week intracortical connections between L4 and L2/3 and within L2/3 (Lendvai, Stern, Chen, & Svoboda, 2000; Stern et al., 2001) are reaching neighboring columns, thereby increasing the probability of cross-columnar activity spread as seen ~P14 in L2/3 (this study and (Wen & Barth, 2011). With the developmental decrease in the amplitude of the late response, the propagation of the late evoked activity to the neighboring column also declined or even vanished (Figure 5d), leaving in P23–27 animals the early response as the main or only activity component for spatio-temporal processing.

4.5 | Developmental profile of MUA evoked by sequential dual-whisker stimulation

We found in barrel cortex of developing mice that sequential deflections of two NW evoked distinct response profiles, depending on the direction and temporal separation of the two stimuli. Neighboring whisker deflection only slightly influenced the PW-evoked MUA in the principal barrel column. A suppression of the evoked response was found in L5 and L6. In contrast, PW deflection suppressed NW-evoked MUA in the principal barrel column. Our findings suggest a developmental increase in surround suppression of whisker-evoked activity due to the functional maturation of inhibitory interneurons to increase lateral inhibition and sharpen the evoked response (Butt, Stacey, Teramoto, & Vagnoni, 2017; Le Magueresse & Monyer, 2013).

4.6 | Association to stimulus coding under active whisking conditions

Although all of the experiments in this study were performed under passive stimulation conditions, several findings could relate to stimulus coding under active whisker conditions. First, the temporal refinement during development should improve phase coding-based object localization (Kleinfeld & Deschênes, 2011). Second, in all layers the PPR at 25-ms ISI increased with development (Figure 4). Along with the progressive reduction in the late response component, this allows the whisker system to better represent consecutive stick-slip events occurring within short succession, as is the case for whisking on sandpaper (Wolfe et al., 2008). Third, the responses to NW stimulation increased with development (Figure 5). This result may indicate that the neural code for texture discrimination in the whisker system might not rely too much on coding whisker identity (Ahissar & Knutsen, 2008). On the other hand, the enhanced response might promote using a latency code (evaluating arrival times of spikes in a given column and in neighboring columns). Thus, a temporal refinement of whisker-evoked responses as described here, in parallel to the onset of active whisking behavior, in our view is consistent with the demand of improved relevant stimulus feature extraction at this developmental stage. Clearly, barrel cortex dynamics during emerging active whisking behaviors warrants further investigations in the future.

4.7 | Potential mechanisms underlying developmental changes

In conclusion, we have shown that during postnatal development sensory processing of single- and dual-whisker stimuli in barrel cortex changes in a layer-specific manner at the onset of whisking behavior. These changes include (a) increased temporal precision in responsiveness; (b) enhanced cross-columnar spread of sensory evoked activity; and (c) sharpening of response specificity to paired and sequential whisker deflections. What mechanisms may underlie these changes? First, these changes temporally coincide with major structural changes at L4-to-L2/3 and L2/3-to-L2/3 synaptic connections (Stern et al., 2001; Wen & Barth, 2011). Second, functional maturation of the neocortical circuitry is modulated by endocannabinoids and neurotrophic factors. Endocannabinoids play an indispensable role on circuit formation of the barrel cortex (Li et al., 2009) and BNDF regulates the development of parvalbumin-containg, fast-spiking interneurons (Itami, Kimura, & Nakamura, 2007). Third, adaptations of the rules for spike-timing-dependent plasticity (STDP) could be important during this developmental period. A developmental

switch of STDP at L4-L2/3 synapses has been reported in mouse barrel cortex between P13 and P15 (with induction of LTP before P13 and induction of LTP or LTD after P15; Itami & Kimura, 2012). This developmental change in the STDP rule may contribute to reorganization of thalamocortical and intracortical circuits (Itami & Kimura, 2016). Interestingly, the switch of STDP is associated with the developmental appearance of thalamus-L2/3 synapses expressing cannabinoid type 1 receptor (Itami et al., 2016). It has been also suggested that GABAergic interneurons may control STDP rules and that GABA acts as switch of Hebbian synaptic plasticity (Paille et al., 2013). Such a mechanism would become operative at the end of the second postnatal week when fast feedforward suppression by prior activation of GABAergic interneurons appears in barrel cortex (Kimura et al., 2010). Given these evidences, we hypothesize that the integration and maturation of GABAergic interneurons during the critical period around P14 modifies STDP rules and further sharpens sensory-evoked activity as reported in our study. Which specific subsets of interneurons are primarily involved in shaping these responses and which other cellular and circuit mechanisms may be at play remain open questions for future studies.

ACKNOWLEDGEMENTS

This work was funded by the German-Swiss Research Unit "Barrel Cortex Function" (DFG FOR1341, SNSF 310030E-147485; F.H. and H.J.L.). We thank Theofanis Karayannis and Christopher Lewis for valuable input on the manuscript.

COMPETING INTERESTS

There are no conflicts of interest to declare.

AUTHOR CONTRIBUTIONS

Conceptualization: AvdB, J-WY, MCS, FH, and HJL; Methodology: AvdB, MCS; Software: AvdB and J-WY; Formal analysis: AvdB, J-WY, VR-P; Investigation: AvdB and J-WY; Writing—original draft: AvdB, J-WY, FH and HJL; Writing—review & editing: MCS, FH, HJL; Visualization: AvdB, J-WY; Supervision: FH and HJL.

DATA ACCESSIBILITY

Data of this study are available upon request from the corresponding author.

ORCID

Heiko J. Luhmann https://orcid.org/0000-0002-7934-8661

REFERENCES

Ackman, J. B., Zeng, H., & Crair, M. C. (2014). Structured dynamics of neural activity across developing neocortex. *bioRxiv*, 012237. https://doi.org/10.1101/012237

Ahissar, E., & Knutsen, P. M. (2008). Object localization with whiskers. *Biological Cybernetics*, *98*, 449–458. https://doi.org/10.1007/s00422-008-0214-4

Arakawa, H., & Erzurumlu, R. S. (2015). Role of whiskers in sensorimotor development of C57BL/6 mice. *Behavioral Brain Research*, *287*, 146–155. https://doi.org/10.1016/j.bbr.2015.03.040

Boloori, A.-R. (2006). The dynamics of spatiotemporal response integration in the somatosensory cortex of the vibrissa system. *Journal of Neuroscience*, *26*, 3767–3782. https://doi.org/10.1523/JNEUROSCI.4056-05.2006

Borgdorff, A. J., Poulet, J. F. A., & Petersen, C. C. H. (2007). Facilitating sensory responses in developing mouse somatosensory barrel cortex. *Journal of Neurophysiology*, *97*, 2992–3003. https://doi.org/10.1152/jn.00013.2007

Brecht, M., Roth, A., & Sakmann, B. (2003). Dynamic receptive fields of reconstructed pyramidal cells in layers 3 and 2 of rat somatosensory barrel cortex. *Journal of Physiology*, *553*, 243–265. https://doi.org/10.1113/jphysiol.2003.044222

Butt, S. J., Stacey, J. A., Teramoto, Y., & Vagnoni, C. (2017). A role for GABAergic interneuron diversity in circuit development and plasticity of the neonatal cerebral cortex. *Current Opinion in Neurobiology*, *43*, 149–155. https://doi.org/10.1016/j.conb.2017.03.011

Campagner, D., Evans, M. H., Loft, M. S. E., & Petersen, R. S. (2018). What the whiskers tell the brain. *Neuroscience*, *368*, 95–108. https://doi.org/10.1016/j.neuroscience.2017.08.005

Capsius, B., & Leppelsack, H. J. (1996). Influence of urethane anesthesia on neural processing in the auditory cortex analogue of a songbird. *Hearing Research*, *96*, 59–70. https://doi.org/10.1016/0378-5955(96)00038-X

Chandrasekaran, S., Navlakha, S., Audette, N. J., McCreary, D. D., Suhan, J., Bar-Joseph, Z., & Barth, A. L. (2015). Unbiased, high-throughput electron microscopy analysis of experience-dependent synaptic changes in the neocortex. *Journal of Neuroscience*, *35*, 16450–16462. https://doi.org/10.1523/JNEUROSCI.1573-15.2015

Chang, M., Suzuki, N., & Kawai, H. D. (2018). Laminar specific gene expression reveals differences in postnatal laminar maturation in mouse auditory, visual, and somatosensory cortex. *Journal of Comparative Neurology*, *526*, 2257–2284. https://doi.org/10.1002/cne.24481

Clem, R. L., & Barth, A. (2006). Pathway-specific trafficking of native AMPARs by in vivo experience. *Neuron*, *49*, 663–670. https://doi.org/10.1016/j.neuron.2006.01.019

Clem, R. L., Celikel, T., & Barth, A. L. (2008). Ongoing in vivo experience triggers synaptic metaplasticity in the neocortex. *Science*, *319*, 101–104. https://doi.org/10.1126/science.1143808

Colonnese, M. T., Kaminska, A., Minlebaev, M., Milh, M., Bloem, B., Lescure, S., … Khazipov, R. (2010). A conserved switch in sensory processing prepares developing neocortex for vision. *Neuron*, *67*, 480–498. https://doi.org/10.1016/j.neuron.2010.07.015

David-Jürgens, M., & Dinse, H. R. (2010). Effects of aging on paired-pulse behavior of rat somatosensory cortical neurons. *Cerebral Cortex*, *20*, 1208–1216. https://doi.org/10.1093/cercor/bhp185

Devonshire, I. M., Grandy, T. H., Dommett, E. J., & Greenfield, S. A. (2010). Effects of urethane anaesthesia on sensory processing in the rat barrel cortex revealed by combined optical imaging and

electrophysiology. *European Journal of Neuroscience*, *32*, 786–797. https://doi.org/10.1111/j.1460-9568.2010.07322.x

Diamond, M. E., von Heimendahl, M., Knutsen, P. M., Kleinfeld, D., & Ahissar, E. (2008). "Where" and "what" in the whisker sensorimotor system. *Nature Reviews Neuroscience*, *9*, 601–612. https://doi.org/10.1038/nrn2411

Durand, S., Iyer, R., Mizuseki, K., de Vries, S., Mihalas, S., & Reid, R. C. (2016). A comparison of visual response properties in the lateral geniculate nucleus and primary visual cortex of awake and anesthetized mice. *Journal of Neuroscience*, *36*, 12144–12156. https://doi.org/10.1523/JNEUROSCI.1741-16.2016

Ego-Stengel, V., Mello e Souza, T., Jacob, V., & Shulz, D. E. (2005). Spatiotemporal characteristics of neuronal sensory integration in the barrel cortex of the rat. *Journal of Neurophysiology*, *93*, 1450–1467. https://doi.org/10.1152/jn.00912.2004

Erchova, I. A., Petersen, R. S., & Diamond, M. E. (2003). Effect of developmental sensory and motor deprivation on the functional organization of adult rat somatosensory cortex. *Brain Research Bulletin*, *60*, 373–386. https://doi.org/10.1016/S0361-9230(03)00060-1

Espinosa, J. S., Wheeler, D. G., Tsien, R. W., & Luo, L. (2009). Uncoupling dendrite growth and patterning: Single-cell knockout analysis of NMDA receptor 2B. *Neuron*, *62*, 205–217. https://doi.org/10.1016/j.neuron.2009.03.006

Feldmeyer, D., Brecht, M., Helmchen, F., Petersen, C. C. H., Poulet, J. F. A., Staiger, J. F., … Schwarz, C. (2013). Barrel cortex function. *Progress in Neurobiology*, *103*, 3–27. https://doi.org/10.1016/j.pneurobio.2012.11.002

Feldmeyer, D., Lübke, J., & Sakmann, B. (2006). Efficacy and connectivity of intracolumnar pairs of layer 2/3 pyramidal cells in the barrel cortex of juvenile rats. *Journal of Physiology*, *575*, 583–602. https://doi.org/10.1113/jphysiol.2006.105106

Feldmeyer, D., Lübke, J., Silver, R. A., & Sakmann, B. (2002). Synaptic connections between layer 4 spiny neurone-layer 2/3 pyramidal cell pairs in juvenile rat barrel cortex: Physiology and anatomy of interlaminar signalling within a cortical column. *Journal of Physiology*, *538*, 803–822. https://doi.org/10.1113/jphysiol.2001.012959

Golshani, P., Gonçalves, J. T., Khoshkhoo, S., Mostany, R., Smirnakis, S., & Portera-Cailliau, C. (2009). Internally mediated developmental desynchronization of neocortical network activity. *Journal of Neuroscience*, *29*, 10890–10899. https://doi.org/10.1523/JNEUROSCI.2012-09.2009

Grant, R. A., Mitchinson, B., & Prescott, T. J. (2012). The development of whisker control in rats in relation to locomotion. *Developmental Psychobiology*, *54*, 151–168. https://doi.org/10.1002/dev.20591

Hara, K., & Harris, R. A. (2002). The anesthetic mechanism of urethane: The effects on neurotransmitter-gated ion channels. *Anesthesia and Analgesia*, *94*, 313–318, table of contents.

Hemelt, M. E., Kwegyir-Afful, E. E., Bruno, R. M., Simons, D. J., & Keller, A. (2010). Consistency of angular tuning in the rat vibrissa system. *Journal of Neurophysiology*, *104*, 3105–3112. https://doi.org/10.1152/jn.00697.2009

Hentschke, H., & Stüttgen, M. C. (2011). Computation of measures of effect size for neuroscience data sets. *European Journal of Neuroscience*, *34*, 1887–1894. https://doi.org/10.1111/j.1460-9568.2011.07902.x

Higley, M. J., & Contreras, D. (2005). Integration of synaptic responses to neighboring whiskers in rat barrel cortex in vivo. *Journal of Neurophysiology*, *93*, 1920–1934. https://doi.org/10.1152/jn.00917.2004

Itami, C., Huang, J.-Y., Yamasaki, M., Watanabe, M., Lu, H.-C., & Kimura, F. (2016). Developmental switch in spike timing-dependent plasticity and cannabinoid-dependent reorganization of the thalamocortical projection in the barrel cortex. *Journal of Neuroscience*, *36*, 7039–7054. https://doi.org/10.1523/JNEUROSCI.4280-15.2016

Itami, C., & Kimura, F. (2012). Developmental switch in spike timing-dependent plasticity at layers 4-2/3 in the rodent barrel cortex. *Journal of Neuroscience*, *32*, 15000–15011.

Itami, C., & Kimura, F. (2016). Concurrently induced plasticity due to convergence of distinct forms of spike timing-dependent plasticity in the developing barrel cortex. *European Journal of Neuroscience*, *44*, 2984–2990. https://doi.org/10.1111/ejn.13431

Itami, C., Kimura, F., & Nakamura, S. (2007). Brain-derived neurotrophic factor regulates the maturation of layer 4 fast-spiking cells after the second postnatal week in the developing barrel cortex. *Journal of Neuroscience*, *27*, 2241–2252. https://doi.org/10.1523/JNEUROSCI.3345-06.2007

Khazipov, R., & Luhmann, H. J. (2006). Early patterns of electrical activity in the developing cerebral cortex of humans and rodents. *Trends in Neurosciences*, *29*, 414–418. https://doi.org/10.1016/j.tins.2006.05.007

Kida, H., Shimegi, S., & Sato, H. (2005). Similarity of direction tuning among responses to stimulation of different whiskers in neurons of rat barrel cortex. *Journal of Neurophysiology*, *94*, 2004–2018. https://doi.org/10.1152/jn.00113.2004

Kimura, F., Itami, C., Ikezoe, K., Tamura, H., Fujita, I., Yanagawa, Y., … Ohshima, M. (2010). Fast activation of feedforward inhibitory neurons from thalamic input and its relevance to the regulation of spike sequences in the barrel cortex. *Journal of Physiology*, *588*, 2769–2787. https://doi.org/10.1113/jphysiol.2010.188177

Kleinfeld, D., & Deschênes, M. (2011). Neuronal basis for object location in the vibrissa scanning sensorimotor system. *Neuron*, *72*, 455–468. https://doi.org/10.1016/j.neuron.2011.10.009

Le Magueresse, C., & Monyer, H. (2013). GABAergic interneurons shape the functional maturation of the cortex. *Neuron*, *77*, 388–405. https://doi.org/10.1016/j.neuron.2013.01.011

Lee, S.-H., & Simons, D. J. (2004). Angular tuning and velocity sensitivity in different neuron classes within layer 4 of rat barrel cortex. *Journal of Neurophysiology*, *91*, 223–229. https://doi.org/10.1152/jn.00541.2003

Lefort, S., Tomm, C., Floyd Sarria, J.-C., & Petersen, C. C. H. (2009). The excitatory neuronal network of the C2 barrel column in mouse primary somatosensory cortex. *Neuron*, *61*, 301–316. https://doi.org/10.1016/j.neuron.2008.12.020

Lendvai, B., Stern, E. A., Chen, B., & Svoboda, K. (2000). Experience-dependent plasticity of dendritic spines in the developing rat barrel cortex in vivo. *Nature*, *404*, 876–881. https://doi.org/10.1038/35009107

Li, L., Bender, K. J., Drew, P. J., Jadhav, S. P., Sylwestrak, E., & Feldman, D. E. (2009). Endocannabinoid signaling is required for development and critical period plasticity of the whisker map in somatosensory cortex. *Neuron*, *64*, 537–549. https://doi.org/10.1016/j.neuron.2009.10.005

Luhmann, H. J., & Khazipov, R. (2018). Neuronal activity patterns in the developing barrel cortex. *Neuroscience*, *368*, 256–267. https://doi.org/10.1016/j.neuroscience.2017.05.025

Luhmann, H. J., & Prince, D. A. (1991). Postnatal maturation of the GABAergic system in rat neocortex. *Journal of Neurophysiology*, *65*, 247–263. https://doi.org/10.1152/jn.1991.65.2.247

Maggi, C. A., & Meli, A. (1986). Suitability of urethane anesthesia for physiopharmacological investigations in various systems. Part 1: General considerations. *Experientia*, *42*, 109–114. https://doi.org/10.1007/BF01952426

Manns, I. D., Sakmann, B., & Brecht, M. (2004). Sub- and suprathreshold receptive field properties of pyramidal neurones in layers 5A and 5B of rat somatosensory barrel cortex. *Journal of Physiology*, *556*, 601–622. https://doi.org/10.1113/jphysiol.2003.053132

Meyer, H. S., Egger, R., Guest, J. M., Foerster, R., Reissl, S., & Oberlaender, M. (2013). Cellular organization of cortical barrel columns is whisker-specific. *Proceedings of the National Academy of Sciences USA*, *110*, 19113–19118. https://doi.org/10.1073/pnas.1312691110

Meyer, H. S., Schwarz, D., Wimmer, V. C., Schmitt, A. C., Kerr, J. N. D., Sakmann, B., & Helmstaedter, M. (2011). Inhibitory interneurons in a cortical column form hot zones of inhibition in layers 2 and 5A. *Proceedings of the National Academy of Sciences USA*, *108*, 16807–16812. https://doi.org/10.1073/pnas.1113648108

Minlebaev, M., Colonnese, M., Tsintsadze, T., Sirota, A., & Khazipov, R. (2011). Early γ oscillations synchronize developing thalamus and cortex. *Science*, *334*, 226–229. https://doi.org/10.1126/science.1210574

Mitzdorf, U. (1985). Current source-density method and application in cat cerebral cortex: Investigation of evoked potentials and EEG phenomena. *Physiological Reviews*, *65*, 37–100. https://doi.org/10.1152/physrev.1985.65.1.37

Nicholson, C., & Freeman, J. A. (1975). Theory of current source-density analysis and determination of conductivity tensor for anuran cerebellum. *Journal of Neurophysiology*, *38*, 356–368. https://doi.org/10.1152/jn.1975.38.2.356

Pagliardini, S., Gosgnach, S., Dickson, C. T., Brown, R., Basheer, R., & McKenna, J., … Morimoto, T. (2013). Spontaneous sleep-like brain state alternations and breathing characteristics in urethane anesthetized mice. *PLoS ONE*, *8*, e70411. https://doi.org/10.1371/journal.pone.0070411

Paille, V., Fino, E., Du, K., Morera-Herreras, T., Perez, S., Kotaleski, J. H., & Venance, L. (2013). GABAergic circuits control spike-timing-dependent plasticity. *Journal of Neuroscience*, *33*, 9353–9363. https://doi.org/10.1523/JNEUROSCI.5796-12.2013

Pammer, L., O'Connor, D. H., Hires, S. A., Clack, N. G., Huber, D., Myers, E. W., & Svoboda, K. (2013). The mechanical variables underlying object localization along the axis of the whisker. *Journal of Neuroscience*, *33*, 6726–6741. https://doi.org/10.1523/JNEUROSCI.4316-12.2013

Peng, Q.-S., Zhou, J., Shi, X.-M., Hua, G.-P., & Hua, T.-M. (2011). Effects of urethane on the response properties of visual cortical neurons in young adult and old cats. *Dongwuxue Yanjiu*, *32*, 337–342.

Quairiaux, C., Megevand, P., Kiss, J. Z., & Michel, C. M. (2011). Functional development of large-scale sensorimotor cortical networks in the brain. *Journal of Neuroscience*, *31*, 9574–9584. https://doi.org/10.1523/JNEUROSCI.5995-10.2011

Reyes-Puerta, V., Sun, J.-J., Kim, S., Kilb, W., & Luhmann, H. J. (2015). Laminar and columnar structure of sensory-evoked multineuronal spike sequences in adult rat barrel cortex in vivo. *Cerebral Cortex*, *25*, 2001–2021. https://doi.org/10.1093/cercor/bhu007

Shen, J., & Colonnese, M. T. (2016). Development of activity in the mouse visual cortex. *Journal of Neuroscience*, *36*, 12259–12275. https://doi.org/10.1523/JNEUROSCI.1903-16.2016

Shimegi, S., Akasaki, T., Ichikawa, T., & Sato, H. (2000). Physiological and anatomical organization of multiwhisker response interactions in the barrel cortex of rats. *Journal of Neuroscience*, *20*, 6241–6248. https://doi.org/10.1523/JNEUROSCI.20-16-06241.2000

Shoykhet, M., Land, P. W., & Simons, D. J. (2005). Whisker trimming begun at birth or on postnatal day 12 affects excitatory and inhibitory receptive fields of layer IV barrel neurons. *Journal of Neurophysiology*, *94*, 3987–3995. https://doi.org/10.1152/jn.00569.2005

Simons, D. J., Carvell, G. E., Hershey, A. E., & Bryant, D. P. (1992). Responses of barrel cortex neurons in awake rats and effects of urethane anesthesia. *Experimental Brain Research*, *91*, 259–272.

Stern, E. A., Maravall, M., & Svoboda, K. (2001). Rapid development and plasticity of layer 2/3 maps in rat barrel cortex in vivo. *Neuron*, *31*, 305–315. https://doi.org/10.1016/S0896-6273(01)00360-9

Tiriac, A., Uitermarkt, B. D., Fanning, A. S., Sokoloff, G., & Blumberg, M. S. (2012). Rapid whisker movements in sleeping newborn rats. *Current Biology*, *22*, 2075–2080. https://doi.org/10.1016/j.cub.2012.09.009

van der Bourg, A., Yang, J.-W., Reyes-Puerta, V., Laurenczy, B., Wieckhorst, M., Stüttgen, M. C., … Helmchen, F. (2017). Layer-specific refinement of sensory coding in developing mouse barrel cortex. *Cerebral Cortex*, *27*, 4835–4850.

Wen, J. A., & Barth, A. L. (2011). Input-specific critical periods for experience-dependent plasticity in layer 2/3 pyramidal neurons. *Journal of Neuroscience*, *31*, 4456–4465. https://doi.org/10.1523/JNEUROSCI.6042-10.2011

Wilent, W. B., & Contreras, D. (2004). Synaptic responses to whisker deflections in rat barrel cortex as a function of cortical layer and stimulus intensity. *Journal of Neuroscience*, *24*, 3985–3998. https://doi.org/10.1523/JNEUROSCI.5782-03.2004

Wolfe, J., Hill, D. N., Pahlavan, S., Drew, P. J., Kleinfeld, D., & Feldman, D. E. (2008). Texture coding in the rat whisker system: Slip-stick versus differential resonance. *PLoS Biology*, *6*, e215. https://doi.org/10.1371/journal.pbio.0060215

Yang, J. W., An, S., Sun, J. J., Reyes-Puerta, V., Kindler, J., Berger, T., … Luhmann, H. J. (2013). Thalamic network oscillations synchronize ontogenetic columns in the newborn rat barrel cortex. *Cerebral Cortex*, *23*, 1299–1316. https://doi.org/10.1093/cercor/bhs103

Yang, J.-W., Hanganu-Opatz, I. L., Sun, J.-J., & Luhmann, H. J. (2009). Three patterns of oscillatory activity differentially synchronize developing neocortical networks in vivo. *Journal of Neuroscience*, *29*, 9011–9025. https://doi.org/10.1523/JNEUROSCI.5646-08.2009

Zehendner, C. M., Tsohataridis, S., Luhmann, H. J., & Yang, J. W. (2013). Developmental switch in neurovascular coupling in the immature rodent barrel cortex. *PLoS ONE*, *8*, e80749. https://doi.org/10.1371/journal.pone.0080749

SUPPORTING INFORMATION

Additional supporting information may be found online in the Supporting Information section at the end of the article.

How to cite this article: van der Bourg A, Yang J-W, Stüttgen MC, Reyes-Puerta V, Helmchen F, Luhmann HJ. Temporal refinement of sensory-evoked activity across layers in developing mouse barrel cortex. *Eur J Neurosci*. 2019;50:2955–2969. https://doi.org/10.1111/ejn.14413